W, Pt, Mo AND Ru ISOTOPE SYSTEMATICS OF IIE IRON METEORITES. M. Fischer-Gödde[1], T. S. Kruijer[1], T. Kleine[1] and J. T. Wasson[2]. [1]Institut für Planetologie, Westfälische Wilhelms-Universität Münster, Wilhelm-Klemm-Str. 10, 48149 Münster, Germany. Correspondence: m.fischer-goedde@uni-muenster.de, [2]Institute of Geophysics and Planetary Physics, University of California, Los Angeles, CA 90095-1567.

Introduction: Group IIE iron meteorites, together with groups IAB-MG and IAB subgroups [1], are classified as non-magmatic iron meteorites. These are distinguished from magmatic iron meteorites in having element-Ni trends that cannot be explained by fractional crystallization [2,3]. They also contain silicate inclusions (in IIE several are chondritic), which are largely absent in members of the magmatic groups. The non-magmatic irons, therefore, are unlikely to be samples of the metal cores of planetesimals, but more likely formed on partially differentiated bodies or within impact-generated melt pools near the surface of undifferentiated asteroids [e.g. 3]. Silicate inclusions in most IIE irons have O isotope compositions similar to H chondrites [4] but three (e.g. Mont Dieu) with chondritic inclusions have $\Delta^{17}O$ values below the H field, consistent with suggestions that these originated on a more reduced and metal rich HH asteroid [5]. A genetic link between IIE irons and H chondrites would be consistent with similar Mo isotope anomalies reported for these two groups of meteorites [6,7]. Metal from IIE irons exhibits higher $^{182}W/^{184}W$ than magmatic iron meteorites, indicating late metal-silicate separation or re-equilibration until up to ~17 Ma after CAI formation [8-10]. Such young Hf-W ages would be consistent with formation of IIE irons from impact-generated melt pools.

The objectives of this study are to constrain the origin and formation history of the IIE iron meteorites through a combined Ru, Mo, Pt, and W isotope study. The aims of our study are (1) to precisely determine metal segregation ages of IIE metal using Hf-W chronometry, and (2) to better constrain the origin of IIE irons and in particular its relation to H chondrites using coupled Mo and Ru isotope analyses. Combined Mo-Ru isotope measurements are an useful tracer of genetic relationships among meteorites, because most meteorites are characterized by distinct and correlated nucleosynthetic Mo and Ru isotope anomalies [6,7,11,12]. However, one caveat when applying high-precision Mo, Ru and W isotope measurements to constrain the formation history of iron meteorites is the presence of cosmic ray-induced neutron cature effects that may have altered the original isotope compositions [12-15]. Determining the indigeneous isotopic composition of iron meteorites to high precision, therefore, also requires an assessment of neutron capture effects for each sample, ideally using Pt isotopes as the neutron dose monitor [12-15]. Here we report Ru, Mo, Pt and W isotope data for 9 IIE iron meteorites (Arlington, Barranca Blanca, Colomera, Kodaikanal, Miles, Mont Dieu, Tarahumara, Watson, and Weekeroo Station) and an H chondrite metal vein (Portales Valley).

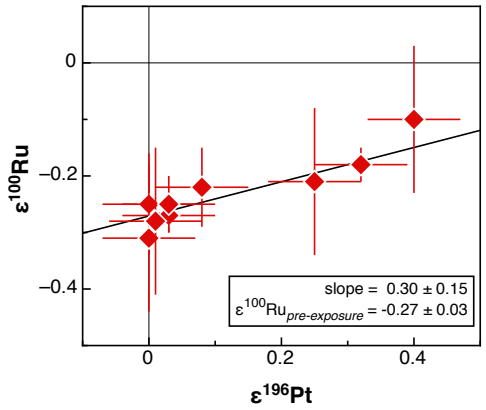

Fig. 1: $\varepsilon^{100}Ru$ vs. $\varepsilon^{196}Pt$ for IIE iron meteorites. The pre-exposure $\varepsilon^{100}Ru$ is obtained from the intercept value at $\varepsilon^{196}Pt = 0$.

Analytical techniques: Iron meteorite (~1 g) were digested in reverse aqua regia in Savillex beakers on a hot plate. After dissolution, aliquots corresponding to ~0.3 g were taken for the separation of Ru, Mo, W, and a ~0.05 g aliquot for Pt. The chemical separation of these elements followed our established protocols [6,12,13]. All isotope measurements were made using the ThermoScientific Neptune *Plus* MC-ICPMS at Münster. The results are reported in ε-units as the parts per 10^4 deviations from terrestrial standard values.

Results: *Platinum:* Measured $\varepsilon^{196}Pt$ values rang from 0.00±0.07 (Kodaikanal) to 0.40±0.07 (Mont Dieu) and indicate variable neutron capture effects in the investigated IIE irons. *Tungsten:* $\varepsilon^{182}W$ values range from -2.23±0.03 (Kodaikanal) to –3.32±0.06 (Mont Dieu). Of note, the samples do not plot on a single correlation line for $\varepsilon^{182}W$ vs. $\varepsilon^{196}Pt$, indicating that the W isotope variations are not only attributable to secondary neutron capture effects. *Ruthenium:* All analyzed samples have negative $\varepsilon^{100}Ru$ between –0.34±0.06 (Portales Valley) and –0.10±0.13 (Mont Dieu). In a plot of $\varepsilon^{100}Ru$ vs. $\varepsilon^{196}Pt$ all samples plot on a single correlation line, indicating neutron capture-induced Ru isotope variations (Fig. 1). *Molybdenum:* $\varepsilon^{92}Mo$ values range from 0.51±0.19 (Colomera) to 1.07±0.20 (Portales Valley).

Discussion: Variations in ε^{196}Pt reflect secondary neutron capture reactions during cosmic ray exposure of the irons and as such can be used to correct for these effects and obtain pre-exposure W and Ru isotope compositions [13-15]. Model ages for metal segregation calculated using the pre-exposure ε^{182}W values reveal that there are at least 3 different age groups among the IIE irons that reflect three different metal segregation events: one group with ages of 3.7-5.3 Ma (Arlington, Barranca Blanca, Colomera and Mont Dieu); a second group with ages of 10-15 Ma (Kodaikanal, Miles, Watson and Weekeroo Station); and Tarahumara with an age of ~27 Ma after CAI formation. For the Portales Valley metal vein we obtained an age of ~11 Ma after CAI formation, perhaps reflecting an impact-induced generation of the metal melt.

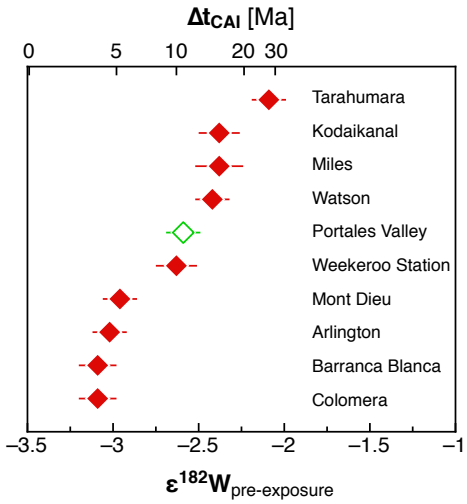

Fig. 2: Pre-exposure ε^{182}W of IIE irons and corresponding model ages of metal segregation.

The pre-exposure ε^{100}Ru of the IIE irons is -0.27±0.03, as obtained from the empirical correlation of ε^{100}Ru and ε^{196}Pt (Fig. 1). This value is indistinguishable from that of ordinary chondrites (-0.30±0.03, [12]) and as such supports a genetic link between IIE irons and ordinary chondrites (Fig. 3). In contrast to Ru, the Mo isotopic composition of the IIE irons seems to be largely unaffected by secondary neutron capture, because ε^{92}Mo values show no correlation with ε^{196}Pt. For instance, the most strongly irradiated IIE Mont Dieu (ε^{196}Pt=0.40±0.07) has the same ε^{92}Mo than the least irradiated IIE irons (e.g., Kodaikanal, ε^{196}Pt~0). Thus, no correction for neutron capture effects is necessary for the Mo isotope data.. The average ε^{92}Mo = 0.75±0.11 obtained for the IIE irons is in very good agreement with previous data for Miles and Watson (0.71±0.24, [6]) and, as shown in Fig. 3, overlaps with ε^{92}Mo = 0.77±0.28 for ordinary chondrites [6]. Moreover, the IIE iron meteorites plot on the cosmic Mo-Ru correlation defined by iron meteorites and chondrites [7]. This correlation indicates the heterogeneous distribution of a single *s*-process carrier at the bulk meteorite scale and as such makes it possible to establish genetical links between different planetary and meteoritic materials. The combined Mo-Ru isotopic data, therefore, provide strong support for earlier conclusions that IIE iron meteorites and ordinary chondrites are genetically linked. These data also show that these two groups of meteorites may also be linked to the IVA iron meteorites (Fig. 3).

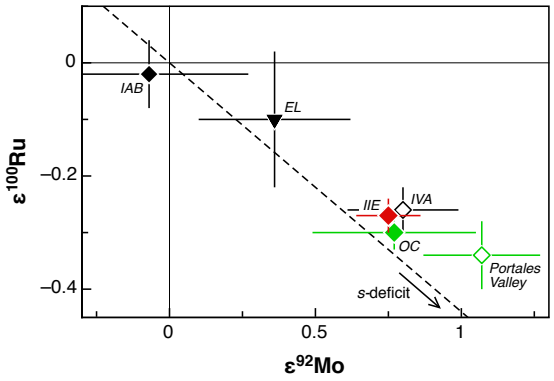

Fig. 3: ε^{100}Ru vs. ε^{92}Mo for IIE, IAB, and IVA iron meteorites, as well as enstatite (EL) and ordinary (OC) chondrites. Dashed line is a calculated mixing line between terrestrial and *s*-process Mo and Ru.

Conclusions: Combined Mo-Ru isotope systematics are consistent with formation of IIE irons by impact melting on an ordinary chondrite parent body. Tungsten model ages for IIE irons reveal at least three different age groups, suggesting that impact events on the IIE parent body occurred separated in time and lasted at least until ~27 Ma after CAI formation.

References: [1] Wasson J.T. and Kallemeyn G.W. (2002) *GCA, 66*, 2445-2473. [2] Scott E.R.D. and Wasson J.T. (1975) *Rev. Geophys. Space Phys.*, 13, 527-546. [3] Wasson J.T. and Wang J. (1986) *GCA, 50*, 725-732 [4] McDermott K.H. et al. (2016) *GCA, 173*, 97-113. [5] Wasson J.T. and Scott E.R.D. (2011) *LPSC 42nd*, #2813. [6] Burkhardt C. (2011) *EPSL, 312,* 390–400. [7] Dauphas N. et al. (2004) *EPSL, 226,* 465–475. [8] Markowski A. et al. (2006) *EPSL, 242*, 1-15. [9] Schersten A. et al. (2006) *EPSL, 341*, 530-542. [10] Qin L. et al. (2008) *EPSL, 273*, 94-104. [11] Chen J.H. et al. (2010) *GCA, 74,* 3851-3862. [12] Fischer-Gödde et al. (2015) *GCA, 168,* 151-171. [13] Kruijer T.S. et al. (2013) *EPSL, 361*, 162-172. [14] Kruijer T.S. et al. (2014) *Science, 344*, 1150-1154. [15] Wittig N. et al. (2013) *EPSL, 361*, 152-161. Schersten A. et al. (2006) *EPSL, 341*, 530-542. Qin L. et al. (2008) *EPSL, 273*, 94-104.